Available online at www.sciencedirect.com
ScienceDirect
Ceramics International 38S (2012) S543–S546
CERAMICS INTERNATIONAL
www.elsevier.com/locate/ceramint

Influence of MgO/CaO ratio on the properties of $MgO–CaO–Al_2O_3–SiO_2$ glass–ceramics for LED packages

Seokju Jang, Seunggu Kang *

Department of Advanced Materials Engineering, Kyonggi University, Suwon 442-760, Republic of Korea

Available online 26 May 2011

Abstract

The crystallization behavior and thermal properties of diopside/cordierite based glass–ceramics fabricated from a $MgO–CaO–Al_2O_3–SiO_2$ (MCAS) glass composition system were studied as a function of the CaO/MgO ratio. The crystallization behavior of the glass–ceramics was investigated in a non-isothermal analysis using a differential thermal analysis performed with various heating rates (5–20 °C/min) and by applying John–Mehl–Avrami and Kissinger equations. The activation energy and Avrami constant were calculated as 332 kJ/mol and 1.0, respectively, indicating that the surface crystallization is preferred. The main peak intensity in the XRD patterns for glass–ceramics is linearly proportional to the thermal diffusivity, density and bending strength. Thus, the crystallinity is, in this case, a more important factor than the ratio of the two crystal phases. The glass–ceramics of CaO/MgO = 1.5 had the highest bending strength of 148 MPa and thermal conductivity of 2.6 W/mk^{-1}due to its high crystallinity.

Keywords: C. Thermal conductivity; C. Thermal expansion; C. Strength; D. Glass ceramics

1. Introduction

A LED(light-emitting diode) package is a device in which the LED chip is built and attached to a printed circuit board(PCB). It is essential to raise the generating power of LED lighting in order to replace general lighting in the several tens to hundreds of watts. The main problem here is to release the heat that is generated. The increased temperature of LED chips due to heat accumulation deteriorates the efficiency and lifetime of the LED chips. To solve this problem, the LTCC(Low Temperature Co-fired Ceramics) concept using the glass–ceramics has been introduced in many studies. A LTCC package fabricated by glass–ceramics process shows a high signal-propagation speed, reliability and chemical durability, a low thermal expansion factor and a low cost [1]. Thus, they have been applied to various modules and substrates, particularly to wireless or microwave devices. In these applications, the sintering of the ceramics should be done at about 950 °C, which is lower than the melting points of copper(1083 °C) or silver(961 °C) [2], which are both potential electrode materials in LTCC.

In this study, the target crystals were selected as diopside and cordierite, and the mother composition system was MCAS ($MgO–CaO–Al_2O_3–SiO_2$) [3]. A small amount of B_2O_3 was added to the mother system to promote densification by a viscous flow caused by the formation with a low melting temperature [4]. Analyses of the thermal properties, crystallization behavior and microstructure were performed as a function of the CaO/MgO. The possibility of applying the diopside/cordierite glass–ceramics fabricated in this study as LED package materials will be investigated.

2. Experimental procedures

The $MgO–CaO–Al_2O_3–SiO_2$ quaternary system was chosen, and the composition of specimens with various CaO/MgO ratios are shown in Table 1. The reagents used were SiO_2(High Purity Chemicals, Japan, 99.9%), Al_2O_3(Samchun Chemicals, Korea, 99%), CaO(High Purity Chemicals, Japan,99.9%), MgO(High Purity Chemicals, Japan,99.9%) and B_2O_3(High Purity Chemicals, Japan,99.9%). For homogeneous mixing of the batch, as shown in Table 1, ball milling for 24 h using zirconia balls was

* Corresponding author. Tel.: +82 31 249 9767; fax: +82 31 244 8241.
E-mail address: sgkang@kgu.ac.kr (S. Kang).

0272-8842/$36.00
doi:10.1016/j.ceramint.2011.05.073

Table 1
The composition of the glass frit (mol%).

Specimen I.D.	3 Major oxides (mol ratio)			Additives (mol%)		CaO/MgO ratio
	SiO_2	CaO	MgO	Al_2O_3	B_2O_3	
CM04	2	0.6	1.4	0.3	0.07	0.42
CM07	2	0.8	1.2	0.3	0.07	0.67
CM10	2	1.0	1.0	0.3	0.07	1.00
CM15	2	1.2	0.8	0.3	0.07	1.50
CM23	2	1.4	0.6	0.3	0.07	2.33

done. The milled batch was melted in an alumina crucible at 1450 °C and for 30 min in an electric furnace and the melted was quenched by pouring it into water. The glass frit obtained was crushed to a particle size of less than 45 μm. A green pellet was formed by a cold isostatic pressing of the glass frit, and this was sintered at 900 °C for 2 h at a heating rate of 10 °C/min.

The glass transition temperature (T_g), crystallization temperature (T_p) and kinetic factor were measured using DTA(-differential thermal analysis, STA 409C/CD, Netzsch Co., Germany) at a various heating rates of 5–20 °C/min. The crystalline phases of the glass–ceramics were identified in a XRD(X-ray diffraction analysis, Pan'alytical, X'pert pro, Netherlands). The microstructures of the glass–ceramics were observed by FESEM (Field Emission Scanning Electron Microscope, JSM-6500F, JEOL Co.) after mirror polishing and etching in a 2 vol% HF solution. The thermal conductivity and thermal expansion coefficient of the glass–ceramics were obtained by a LFA (laser flash apparatus, Netzsch Co., Germany) and a dilatometer (DIL 402C, Netzsch Co., Germany), respectively. The three-point bending strength of a glass–ceramics of 15 mm × 8 mm × 5 mm was performed with a span of 10 mm at a cross-head speed of 5 mm/min.

3. Results and discussion

The DTA curves with various heating rates for stoichiometric composition glass (CM10) were analyzed, as shown in Fig. 1, to investigate the crystallization behavior and kinetic factor. The positions of the exothermic and endothermic peak were found to shift toward a higher temperature with the intensities of each peaks were increased heating rate.

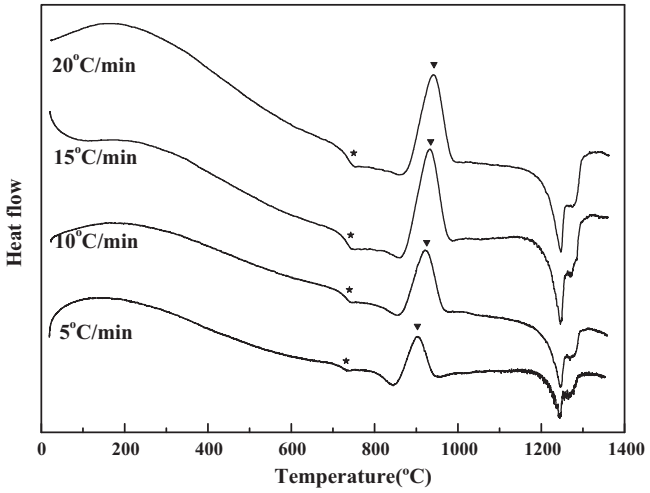

Fig. 1. DTA curve with various heating rates of the CM10 to calculate the activation energy.

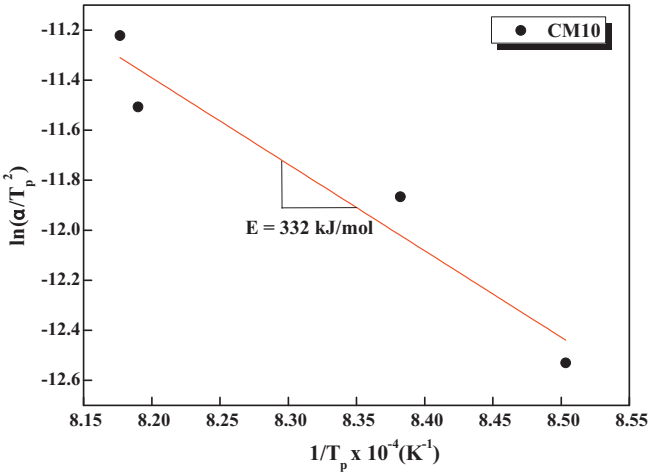

Fig. 2. Kissinger plot for (α/T_p^2) vs. (a/T_p) of the CM10.

The activation energy(E) and the Avrami constant(n) are important factors in analysis of the crystallization behavior of glass. The activation energy for crystallization can be calculated by the Kissinger Eq. (1) as follows [5]:

$$\ln\left(\frac{\alpha}{T_p^2}\right) = \left(\frac{-E}{RT_p}\right) + \text{constant} \quad (1)$$

here, T_p is the crystallization temperature at a given heating rate, R is the gas constant, and α is the heating rate.

The activation energy can be calculated from the slope of a linear curve relating (α/T_p^2) vs. ($1/T_p$) as shown in Fig. 2. The activation energy was calculated as approximately 332 kJ/mol. The activation energy for crystallization from glass is known to range from 200 kJ/mol to 400 kJ/mol. Generally, the higher the activation energy E a given crystalline phase, the more energy is needed to grow this crystal and hence the more difficult it is to grow it three-dimensionally [6]. Consequently, the surface crystallization is dominant rather than the bulk crystallization for crystals with higher activation energy.

The Avrami constant, n, can be determined from the Augis–Bennett Eq. (2) as follows [7]:

$$n = \left(\frac{-E}{\Delta T_{FWHM}}\right) \times \left(\frac{RT_p^2}{E}\right) \quad (2)$$

In this equation, ΔT_{FWHM} denotes the width of the exothermic peak the DTA curve. A crystallization value of n

Table 2
Glass transition and crystallization temperature (heating rate = 10 °C/min).

	T_g (°C)	T_{p1} (°C)	T_{p2} (°C)
CM04	750	950	–
CM07	743	936	–
CM10	740	948	–
CM15	742	951	1040
CM23	750	955	1020

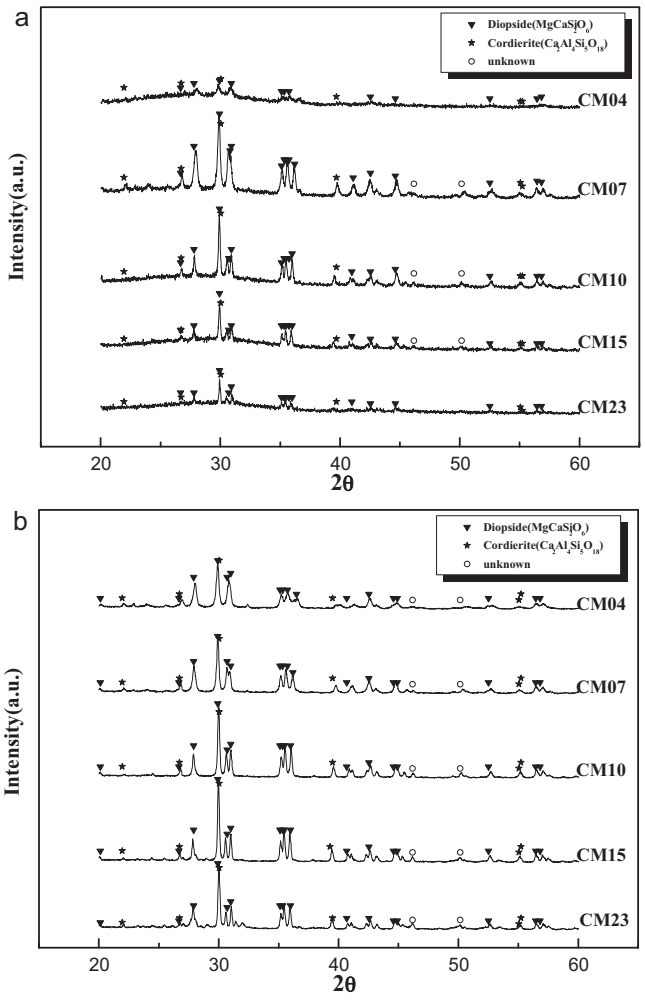

Fig. 3. XRD patterns of glass–ceramics sintered at (a) 850 °C and (b) 900 °C for 2 h.

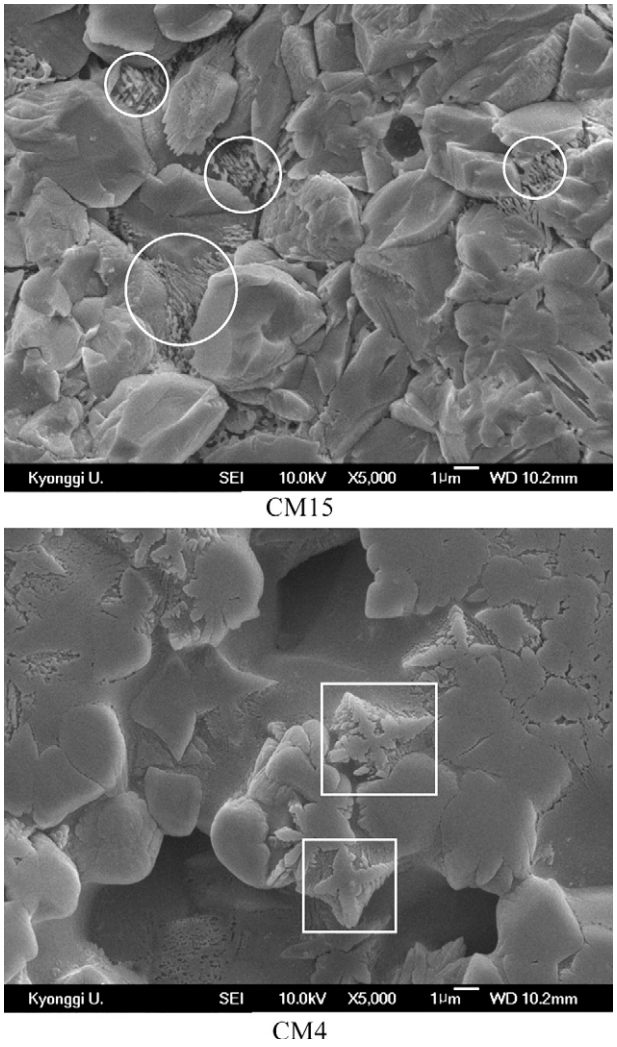

Fig. 4. Comparison of CM15 and CM4 glass–ceramics in terms of their microstructure observed by SEM after sintering at 900 °C for 2 h.

close to 3 is known as favoring bulk or three-dimensional crystallization, whereas surface nucleation is for values close to 1 [8].

The DTA result, obtained at heating rate of 10 °C/min, is shown in Table 2. The glass transition temperature and crystallization temperature increase as the CaO/MgO ratio increases. In addition, the crystallization temperatures for all specimens were under 1000 °C, which is low enough for a LTCC process application.

All of the specimens sintered at 800 °C were amorphous, as identified from the X-ray diffraction patterns. Most of the specimens except CM04, sintered at 850 °C and 900 °C for 2 h, had a diopside and cordierite crystalline phase, as shown in Fig. 3. The crystallization intensity sintered at 850 °C for 2 h decreased as the CaO/MgO ratio increased except for CM4. The major phase of the glass–ceramics sintered at 900 °C for 2 h was diopside, and CM15 had the highest intensity, while CM4 had the lowest peak intensity of diopside among all glass–ceramics sintered at 900 °C, as shown Fig. 3(b).

The microstructures of the glass–ceramics of CM15 and CM4 sintered at 900 °C are compared in Fig. 4. This figure shows that a considerable amount of liquid formed in the CM4 glass–ceramics. Needle-like crystals (□) were stopped up between the crystal particles in the CM15 specimen, resulting in increased densification. Moreover, some dendrite crystals (○) were observed in the CM4 sample. Generally, a dendrite-shaped crystal is generated when the activation energy for the crystal growth is low and the latent heat is high [9].

The physical properties of glass–ceramics with various CaO/MgO ratios sintered at 900 °C for 2 h are shown in Table 3.

Table 3
Various properties of the glass–ceramics sintered at 900 °C for 2 h.

	CM04	CM07	CM10	CM15	CM23
Thermal conductivity (W/mK)	1.8	1.6	1.9	2.6	1.7
Density (g/cm^3)	2.78	2.77	2.82	2.83	2.84
Thermal diffusivity (mm^2/s)	0.74	0.71	0.86	0.93	0.85
Specific heat capacity (J/gK)	0.82	0.79	0.79	0.77	0.72
Coefficient of thermal expansion (10^{-6}/K)	16.85	18.06	15.21	8.52	16.24
Bending strength (MPa)	132	134	145	148	138

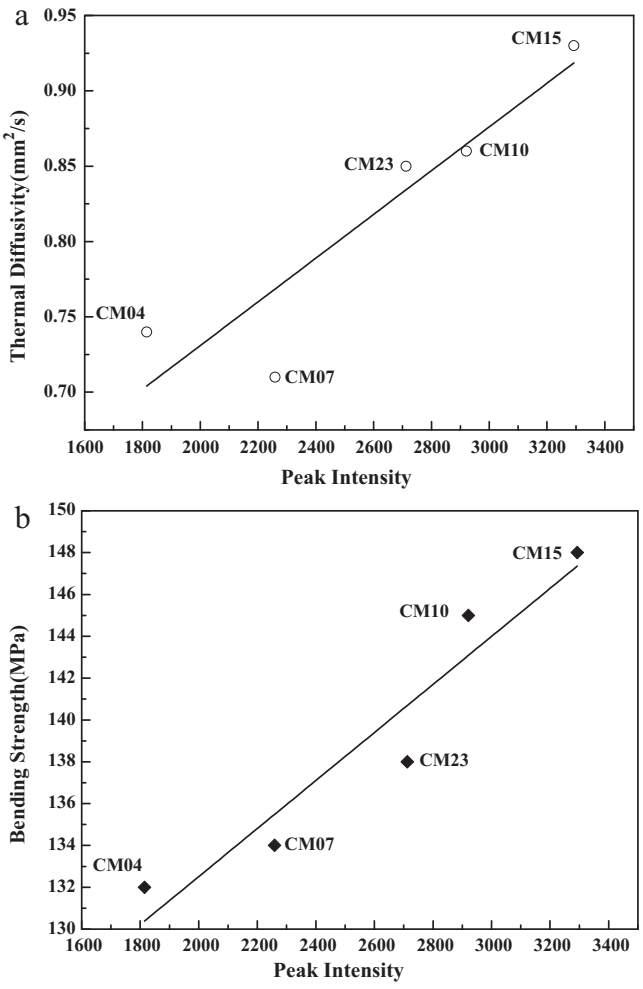

Fig. 5. Peak intensity vs. thermal diffusivity and bending strength of glass–ceramics of diopside and cordierite base showing the linear proportion relationship.

CM15 had the highest bending strength, thermal conductivity and thermal diffusivity, as well as the lowest coefficient of thermal expansion among the all specimens due to its high crystallinity.

The main peak intensity in the XRD patterns for glass–ceramics is linearly proportional to the thermal diffusivity and bending strength, as shown in Fig. 5. Consequently, the crystallinity is, in this case, a more important factor than the ratio of the two crystal phases.

4. Conclusions

Glass–ceramics composed of diopside and cordierite were fabricated from a MgO–CaO–Al_2O_3–SiO_2 glass composition system and their crystallization behavior, microstructure and properties with various CaO/MgO ratios were analyzed. The activation energy and Avrami constant of stoichiometric composition of diopside(CaO/MgO = 1.0), were found to be 332 kJ/mol and 1.0, respectively, indicating that surface crystallization was dominant.

The all specimens sintered at 800 °C were amorphous. Most of the specimens sintered at 850 °Cexcept specimen of CaO/MgO = 0.4 had a diopside and a cordierite phase. The major phase of the glass–ceramics sintered at 900 °C was diopside, and the microstructure developed was composed of crystal particles packed with needle-like crystals. The specimen of CaO/MgO = 1.5 sintered at 900 °C for 2 h showed the lowest thermal expansion coefficient ($8 \times 10^{-6}\ K^{-1}$) and the highest three-point bending strength (148 MPa), thermal diffusivity (0.93 mm^2/s) and thermal conductivity (2.6 W/mk^{-1}) among all specimens owing to its high crystallinity.

References

[1] R.R. Tummala, Ceramics and glass ceramics packaging in 1990s, Journal of the American Ceramic Society 74 (5) (1991) 895–908.
[2] V.M.F. Marques, D.U. Tulyaganov, J.M.F. Ferreira, Low temperature synthesis of anorthite based glass–ceramics via sintering and crystallization of glass-powder compacts, Journal of the European Ceramic Society 26 (2006) 2503–2510.
[3] T.I. Barry, L.A. Lay, R. Morrell, High temperature mechanical properties of cordierite refractory glass ceramic, Journal of the British Ceramics Society 25 (1975) 67–84.
[4] F.J. Torres, E. Ruiz de Sola, J. Alarcon, Effect of boron oxide on the microstructure of mullite-based glass ceramic glazes for floor-tiles in the CaO–MgO–Al_2O_3–SiO_2 system, Journal of European Ceramic Society 26 (2006) 2285–2292.
[5] H.E. Kissinger, Reaction kinetics in differential thermal analysis, Analytical Chemistry 29 (11) (1957) 1702–1706.
[6] H.S. Kim, The crystallization kinetics of CaO–MgO–Al_2O_3–SiO_2 glass system using thermal analysis, Journal of the Korean Ceramic Society 29 (1) (1992) 9–14.
[7] J.A. Augis, J.D. Bennett, Calculation of the Avrami parameter from heterogeneous solid state reaction using a modification of Kissinger method, Journal of the Thermal Analysis 13 (2) (1978) 283–287.
[8] S. Jang, S. Kang, Microstructural analysis for hybrid materials composing of nepheline crystal and glass matrix fabricated from coal bottom ash, Journal of the Ceramic Processing Research 10 (2009) 59–63.
[9] S. Kang, Effect of modifiers on the properties of glass–ceramics containing coal bottom ash, Journal of the Korean Crystal Growth 20 (1) (2010) 53–57.